Posture Estimation of Curve Running Motion Using Nano-Biosensor and Machine Learning

Xiaoming Wu[1], Yu Cao[2], Yu Wang[1]*, Bing Li[3], Haitao Yang[4], S. P. Raja[5]

[1] Department of Physical Education, Capital Normal University, Beijing 100048 (China)
[2] Physical Education Department, Renmin University of China, Beijing100872 (China)
[3] College of Physical Education and Training, Harbin Sport University, Harbin 150008 (China)
[4] Physical Education Department, Beijing University of Technology, Beijing 100124 (China)
[5] School of Computer Science and Engineering, Vellore Institute of Technology, Vellore 632014, Tamilnadu (India)

* Corresponding author: wangyuwy2022@126.com

Abstract

Curve running is a common form of training and competition. Conducting research on posture estimation during curve running can provide more accurate training and competition data for athletes. However, due to the unique nature of curve running, traditional posture estimation methods neglect the temporal changes in athlete posture, resulting in a decrease in estimation accuracy. Therefore, a posture estimation method for curve running motion using nano-biosensor and machine learning is proposed. First, the motion parameters of humans are collected by nano-biosensor, and the posture coordinates are obtained preliminarily. Second, the posture coordinates are established according to the human motion parameters, and the curve running posture data is obtained and filtered to obtain more accurate data. Finally, the Bayesian network in machine learning is used to continuously track the posture, and a nonlinear equation is established to fuse the posture angle obtained by the sensor and the posture tracked by the Bayesian network, to realize the posture estimation of curve running motion. The results show that the proposed estimation method has a good motion posture estimation effect, and the hip joint estimation error, knee joint estimation error and ankle joint estimation error are all less than 5°, and the endpoint displacement estimation offset rate is less than 2%. It can realize accurate motion posture estimation of curve running motion, and has important application value in the field of track training.

Keywords

I. Introduction

Curve running is one of the most important activities of human beings in daily life/social interaction/production, which reflects the difference in individual physical quality to a certain extent [1]. At the same time, it is also a basic event in track and field sports, playing a very important role in the development of human speed, agility, endurance, coordination, etc. Running can promote the growth and development of the body, improve the cardiopulmonary function, and enhance the physical quality of people. And the curve running estimation of athletes can help timely find the shortcomings of athletes, and then guidance can be provided to improve the athletes' sports level [2]. Posture estimation refers to the process of accurately determining and analyzing the body's position and alignment in a given context or activity. In the case of curve running, posture estimation involves precisely identifying and tracking the positions and movements of the athlete's body during the running process, especially during the turns [3]-[4]. Motion posture estimation is a key content in the current computer vision research field [5]-[6]. However, traditional posture estimation methods are not sufficient to meet the high-precision and high-efficiency posture estimation needs of curve runners. Therefore, it is necessary to conduct posture estimation research specifically for curve running. During the process of curve running, the posture of athletes changes continuously over time, and there is a significant posture change during turning, which brings great challenges to posture estimation [7]. Furthermore, due to the rapid and complex nature of athlete posture changes, traditional posture estimation methods cannot accurately capture posture changes, resulting in a decrease in estimation accuracy. Therefore, a curve running posture estimation study is proposed using nano-biosensors and machine learning. Nano-biosensors are biosensors based on nanotechnology. Their main function is to detect and analyze small biological systems, such as biological molecules or cells. Typically, nano-biosensors consist of nanomaterials, biological recognition elements, and transducers.

By utilizing the special properties of nanomaterials, nano-biosensors can achieve high-sensitivity detection of trace amounts of biological molecules, while also having advantages such as high selectivity, rapid response, miniaturization, and low cost, making them widely applicable in fields such as medical diagnosis, food safety testing, and environmental monitoring [8]-[9].

The traditional biosensors used for human motion posture analysis are based on optical detection. Nano-biosensors include optics, electricity, mechanics, acoustics, and so on. They are not only sensitive and fast, but also portable and have low energy consumption, becoming one of the preferred technologies for human motion posture analysis [10]. The combination of nano-biosensors and vision-based machine learning can create a digital version of the human posture of curve running in real- time, and a virtual and real interactive three-dimensional (3D) environment is generated. It provides a basis for the study of the posture estimation of curve running. In addition to its benefits for athletes, curve running and its posture estimation have broader implications for the general population. Running, as a form of exercise, promotes overall physical fitness, enhances cardiopulmonary function, and contributes to the growth and development of the body. By accurately estimating curve running postures, the proposed nano-biosensor and machine learning approach can help individuals improve their running techniques, prevent injuries, and optimize their training regimen. Furthermore, the combination of nano-biosensors and machine learning not only provides real-time posture estimation but also generates a virtual and interactive 3D environment. This immersive environment allows athletes, coaches, and researchers to analyze and visualize the runner's movements from different perspectives. By examining and manipulating this digital representation, athletes can gain a deeper understanding of their running form, identify areas for improvement, and experiment with different strategies in a risk-free virtual setting [11]-[12].

At present, some scholars have studied motion posture estimation methods. In which, Shimada et al.[13] studied the method of 3D human motion capture and posture estimation with physical consciousness. The proportional differential controller is introduced, whose gain is predicted by the neural network, which can reduce the delay even in the case of fast motion, to realize the construction of human motion capture architecture. According to the results of monocular 3D human motion capture, the neural network is standardized based on physical awareness. This makes it possible to estimate the global translation more accurately without loss of generality, and use the trained neural network model to estimate the motion posture. The experimental results show that this method has the problem of poor motion posture estimation effect, and it is difficult to achieve the relevant expected goals. Gao et al.[14] studied the motion posture estimation method based on wireless wearable technology. Wireless wearable sensors are used to collect human motion data, and the collected data format is processed accordingly. The features of different posture signals are studied, and the signal feature sequence that can identify the signal posture is selected. According to the signal feature sequence of the posture in the posture database, a multi-level human posture estimation algorithm is designed, and the human motion posture estimation results are obtained. The analysis of the test results shows that the method has high estimation error and poor estimation accuracy for hip joint posture. Liu et al. [15] studied the human motion posture estimation method of RGB-D sensor, and designed a human motion capture system combining human priori and performance capture. This system only uses a single RGB-D sensor. To break the self-scanning constraint, the front view input is used to initialize geometric capture to ensure the quality of human motion capture. Based on the motion capture results, a human motion posture estimation model is built to obtain the human motion posture estimation results. However, this method has a high error in estimating the knee joint posture, making it difficult to accurately estimate the posture of curve running, and the actual application effect is poor. Liu et al. [16] studied the motion posture estimation method based on micro-inertial measurement unit (MIMU). By combining micro flow sensor with MIMU, a wearable flow MIMU human motion capture device is pro-postured. The motion speed is detected by the micro flow sensor and used to calculate the motion acceleration. The gravitational acceleration is extracted by eliminating the motion acceleration from the accelerometer output. Posture estimation is realized by fusing the gyro output of the Kalman filter and the extracted gravity acceleration data. This method needs better estimation error for ankle joint posture, resulting in low estimation accuracy, which affects its further promotion in practice. Chen and Li [17] studied the motion posture estimation method based on semi-supervised learning. First, the Internet of Things is used to collect human motion target images, extract human motion posture features based on the eight-star model, and fuse multiple features to form a 17-dimensional feature vector image block. Then, the random fern classifier is optimized, and semi-supervised learning is used to calculate a large number of un-calibrated data in the time domain, space domain and data. The classifier is trained to complete the image block classification. Finally, classifier's parameters are updated iteratively to complete the posture estimation of moving human objects. However, this method has the problems of a high offset rate of terminal displacement estimation, low accuracy of posture estimation and poor practical application effect.

To address the problem of poor posture estimation effect, high hip joint estimation error, knee joint estimation error, ankle joint estimation error and endpoint displacement estimation offset rate in traditional motion posture estimation methods, combined with the advantages of nano-biosensor and Bayesian network[18], it is applied to curve running motion posture estimation to improve the estimation effect. The main contributions of this paper are as follows:(1) Nanometer biosensor has the advantages of high sensitivity and wide detection range, which can improve the speed and quality of athletes' initial posture acquisition, and solve the problem of rising posture estimation error caused by poor quality of athletes' initial posture acquisition.(2) The Bayesian network is used to track the posture, and all the postures are fused to ensure the depth estimation of the hip joint, knee joint, ankle joint and other postures, and ensure the accuracy of posture estimation. (3) experiment's results using different data sets prove that the proposed method of curve running posture estimation using nano-biosensors and machine learning can achieve fast and accurate estimation of curve running posture.

II. Methodology

A. Design of Posture Estimation Method for Curve Running

To address the issues of poor posture estimation, high hip joint estimation error, knee joint estimation error, ankle joint estimation error, and high endpoint displacement estimation offset rate in traditional motion posture estimation methods, the advantages of nano-biosensors and Bayesian networks are combined and applied to the curve running motion posture estimation to improve estimation effectiveness. The central idea of this research method is to use nano-biosensor to obtain the initial posture of a motion, get the solution, and use machine learning methods to continuously track and calculate, to achieve the posture estimation, as shown in Fig. 1.

The nano-biosensor is installed in the appropriate position to obtain the athletes' initial posture information and determine whether the posture calibration is completed. After the posture calibration meeting, the posture data is obtained and filtered. After initial alignment and solution, the posture angle is obtained to obtain more accurate data.

The Bayesian method in machine learning is used to continuously track the posture. After the pre-training is completed, a nonlinear equation is established to fuse the posture angle obtained by the sensor with the posture tracked by the machine learning method, and the posture estimation result of the curve running motion is output.
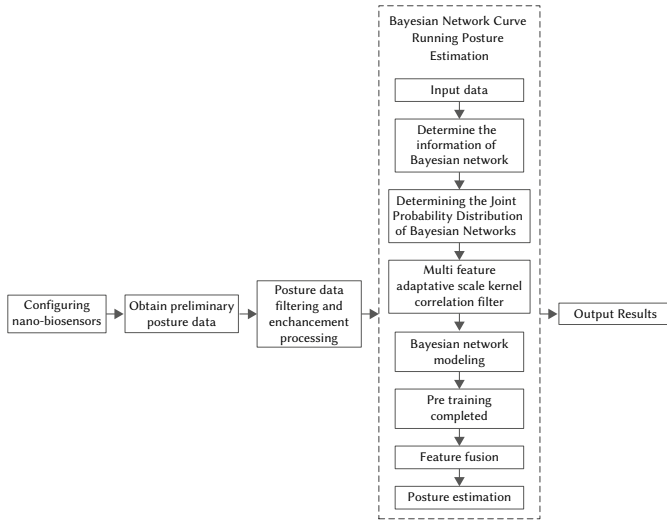

Fig.1. Framework of estimation Process of Curved Running Posture.

B. Posture Coordinate Acquisition Based on Nano-Biosensor

In this paper, Nano-biosensor is used to collect human motion parameters and preliminarily obtain posture coordinates. Nano-biosensor is a new type of biological sensing medium using nanomaterials. Compared with inertial sensor-based data acquisition methods, it has advantages in the field of biological data acquisition because of its small device size, free labeling, good specificity, and high data acquisition efficiency. It consists of Nano recognition element, transducer, and an electronic instrument. The nano-biosensor is installed on the subject, the data acquisition site is determined, and the collected electrical signal or optical signal is transmitted to the computer through wireless communication, and the signal is amplified and processed to ensure the data acquisition accuracy and efficiency.

The nano-biosensor is used to collect human motion parameters. The position of the sensor determines whether the posture information of different bones and joints can be accurately obtained. There are 206 bones in the human body, and all bones are connected to human skeleton by joints of different forms [19]. In this study, a skeleton model with 15 rigid bodies is used for posture measurement. The sensor is worn on these 15 parts. The fixing position is shown in Fig. 2.
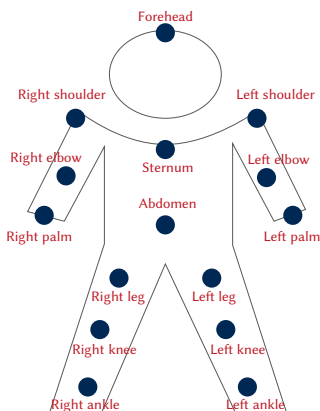

Fig.2. Fixed position of sensor.

Binding the sensor to each joint-driven bone enables the specific biometric information captured to be converted into easily detectable physicochemical signals, such as optical and electrical signals, and the rotation information of the joint is determined by the associated biological signals. For further analysis, mathematical language is used to describe the human skeleton and calculate the posture of each sensor unit [20]. In the sensor coordinate system, the three-axis acceleration vector output by the accelerometer is recorded $[u_x, u_y, u_z]$, and the acceleration vector obtained after integration is recorded as $[v_x, v_y, v_z]$. In an ideal state, these two groups of acceleration vectors are equal [21]. However, in the measurement, it is inevitable to be affected by the system error and the installation error of the device itself, resulting in that they are not completely equal. Therefore, the two vectors are multiplied to calculate the error I. Equation (1) refers to

$$I = \begin{bmatrix} u_x \\ u_y \\ u_z \end{bmatrix} \times \begin{bmatrix} v_x \\ v_y \\ v_z \end{bmatrix} = \begin{bmatrix} u_y v_z - u_z v_y \\ u_z v_x - u_x v_z \\ u_x v_y - u_y v_x \end{bmatrix} \tag{1}$$

During posture solution, the angle is the rotation around the axis z, i.e., to form an intersection angle on the plane xoy.

After the above preparation, the initial posture is determined by using the three-axis measurement values [22]. After the initial posture matrix of the motion is determined [23], the initial alignment is completed. Equation (2) and Equation (3) refer to

$$\theta = arcsin\left(-\frac{k_y}{k}\right) \tag{2}$$

$$\gamma = arctan\left(-\frac{k_x}{k_z}\right) \tag{3}$$

where $[k_x, k_y, k_z]$ represents each angle parameter in the coordinate system. θ and γ represent pitch angle and roll angle, respectively.

The euler angle can represent any 3D coordinate curve. Therefore, this method is used to describe the carrier posture angle [24], and the sum of rotation angles is

$$\varpi = (\varphi + \alpha + \beta + \theta + \gamma) \cdot I \tag{4}$$

where φ, α and β are the rotation angle vectors of heading axis, pitch axis and roll axis.

The three angle values calculated above represent the orientation information of the motion. However, the posture angle obtained based on the nano-biosensor is only fixed. Since the motion posture of curve running is real-time, it needs to be tracked in real-time for further processing.

C. Data Filtering of Curve Running Posture

Using nano-biosensor to collect human motion parameters, the initial posture coordinates is obtained, and the posture data of curve running are obtained. Because the detection object is constantly moving, it is necessary to estimate the curve running posture. Therefore, there will be some errors in the detection. It is necessary to filter and enhance the data [25] to avoid excessive bridging of the model and improving the accuracy of the motion posture description.

The sample database is defined as D, the spatial position of human joints is recorded as $l(x, y)$, and the goal is to filter the motion posture data of curve running. In the whole process, the random gradient descent method [26] is used to iterate and update the algorithm. Equation (5) refers to

$$S_{t+1} = A_t + \gamma_t \cdot \sum_{(x,y) \in D_t} [l(x, y)] \tag{5}$$

where S_{t+1} is the updated sample data set. A_t represents a sample set randomly selected from the database, γ_t represents the gradient value of the loss function within the time t, and D_t represents the target function of the identification performance.

Data filtering is realized through an additional random sampling process to enhance the effect on each small batch of collected samples. Polynomial distribution is adopted for the training samples to be disturbed. Equation (6) refers to

$$P(S_{t+1}) = 1 - \frac{c-1}{c} * \partial * h \tag{6}$$

where ∂ refers to the possibility for different categories to emerge. c is the error ratio, and h means the category of the real label.

The distribution of training data is obtained through the above calculation. If c is 0, the sample does not include error data; if c is 100%, most of the labels are abandoned, and the training process is close to unsupervised. Each iteration is trained on different noise samples relative to the model, and the data filtering process will be ended until all samples are trained.

D. Posture Estimation of Curve Running Based on Bayesian Network

After the above Data filtering processing, the Bayesian network in machine learning is used to continuously track the posture and realize motion posture estimation. In machine learning, there are two known variables, which are recorded as m and n. There is a certain dependency between the two variables, that is, there is an unknown joint probability distribution $H(m, n)$. Machine learning estimates the maximum a posteriori probability based on l different samples.

In the actual calculation, it is assumed that the data obey the Gaussian distribution, and a radial basis function is used to represent the data association [27]. Because the joint distribution prior has the characteristics of Gaussian distribution, the posterior prediction output value $B(y^{(c)})$ of new data is expressed as

$$B\left(y^{(c)}\right) = y^{(c)} G_Z^{-1} D_X \tag{7}$$

where $y^{(c)}$ is a posteriori prediction parameter, G_Z^{-1} is the observation value of the vector Z, and D_X is the hidden structure associate parameter of the data X.

Track the target after obtaining the posterior predictive output value. Scale Adaptive with Multiple Features Tracker is a scale adaptive kernel correlation filter tracker with feature fusion. Aiming at the problem of fixed template size in tracking, an adaptive scheme is proposed [28]. The image target of the previous frame is taken as the processing center, and the image blocks in the matrix area around the processing center target are recorded m x n. Process all cyclic block shifting. Equation (8) refers to

$$k = \left[-\frac{1}{u^2}(e^2 + e'^2) - 2P^{-1}\right] \cdot B\left(y^{(c)}\right) \tag{8}$$

where u is bandwidth parameter of Gaussian kernel function, e is offline Fourier transform parameter, and P is scale transformation parameter.

To combine the motion posture obtained from biosensors with the tracking and measurement equation based on machine learning [29], it is necessary to establish a nonlinear equation to update the motion posture estimation [30]. When changes occur, one of the coordinate systems shall be translated in advance. Equation (9) refers to

$$J(j_0, j_1, j_2, j_3) = j_0 + j_1 i + j_2 j + j_3 k \tag{9}$$

where $J(j_0, j_1, j_2, j_3)$ represents the coordinate system after translation. j_0, j_1, j_2 and j_3 are unit vectors.

Under $J(j_0, j_1, j_2, j_3)$ coordinate system. The angular change within the same sampling time interval is called angular increment [31]. Equation (10) refers to

$$C = q \cdot C(t_k) \tag{10}$$

where $C(t_k)$ is the incremental value at moment t, and q is the sampling time interval.

According to the transformation relationship in the posture fusion coordinate system [32], the geographic coordinate system and the carrier coordinate system are transformed to further describe the posture information in motion. Equation (11) refers to

$$a = \begin{bmatrix} a_x \\ a_y \\ a_z \end{bmatrix} = B \begin{bmatrix} -2(h_1 h_3 - h_0 h_2) \\ -2(h_2 h_3 + h_0 h_1) \\ -h_0^2 + h_1^2 + h_2^2 - h_3^2 \end{bmatrix} \tag{11}$$

where a represents the attitude angle after conversion. h_0, h_1, h_2 and h_3 represent posture angle vector, respectively, and B represents conversion parameter.

According to the nonlinear state equation [33], the relationship between the measurement equation and the state equation can be obtained by processing the measured data with the Jacobian matrix. The Jacobian matrix is in the form of

$$O_a = \frac{\partial a}{\partial h} = \begin{bmatrix} 2h_2 & -2h_3 & 2h_0 & -2h_1 \\ -2h_1 & -2h_0 & -2h_3 & -2h_2 \\ -2h_0 & 2h_1 & 2h_2 & -2h_3 \end{bmatrix} \tag{12}$$

Finally, the loss function is used to recover the 3D human posture, and the final estimation results are obtained

$$W = O_a[A_t(\theta) + A_a(\theta)] \tag{13}$$

where $A_t(\theta)$ represents the action-angle of node A at time t. $A_a(\theta)$ stands for A unit parameter at joint point α.

Based on obtaining the posture angle, the motion trend is tracked continuously, and the posture estimation of curve running is completed.

III. Experimental Analysis and Results

A. Data Sets

A total of two data sets are used for comparative experiments, namely, MS COCO data set [34] and actual collection data set, which are recorded as data set 1 and data set 2. Data set 1: MSCOC data set is large in scale, including many scenes such as target detection, segmentation, image description, and so on. The target category is diverse, and contains many different human motion pose images. It is a dataset specially used for image recognition. The dataset contains 91 classifications, 82 of which each have more than 5000 instance objects. Data set 2: The second dataset is collected data. The experimenter hung the sensor on his waist and ran according to different habits. Since the limit frequency of human daily movement is within 100Hz, this experiment samples at 100Hz, and 18000 sample data can be obtained for each posture. The data set covers 10 human activities, and the test objects of each activity include 50 men and 50 women. Each image has activity labels and human joints are labeled. Selecting 625 experimental images from two datasets, each with multiple angles, different speeds, and positions, the images were preprocessed before experimenting. During the experiment, 80% of the randomly selected data samples were experimental, while 20% were test samples. All data were input into the computer for experimental analysis. The Bayesian network model was used. The number of neurons in each node was adjusted according to specific circumstances to achieve optimal performance. The learning rate was set to 0.1 to control the convergence speed of the model and avoid overfitting or under-fitting situations.

1. Evaluation Metrics

Motion posture estimation effect: The closer the posture angle calculated by different methods is to the actual athlete's posture angle, the better the estimation effect is. Equation (14) refers to

$$K = |K_i - K_j| \tag{14}$$

where K_i is the posture angle calculated by different methods, and K_j is the posture angle of an athlete in reality.

where is the posture angle calculated by different methods, and K_j is the posture angle of an athlete in reality.

Hip joint estimates: The closer the estimated result of knee joint angle is to the actual result, the better the estimated effect is. Equation (15) refers to

$$g = |g_i - g_j| \tag{15}$$

where, g_i is the hip joint angle estimation results calculated by different methods, and g_j is the athlete's actual hip angle.

Knee joint estimates: The closer the estimated result of knee joint angle is to the actual result, the better the estimated effect is. Equation (16) refers to

$$h = |h_i - h_j| \tag{16}$$

where h_i is knee joint angle estimation results are calculated by different methods, and h_j is the athlete's actual knee joint angle.

Ankle joint estimates: The closer the ankle angle estimation result is to the actual result, the better the estimation effect is. Equation (17) refers to

$$z = |z_i - z_j| \tag{17}$$

where z_i is the angle estimation results of ankle joint calculated by different methods, and z_j is the athlete's actual ankle joint angle.

Endpoint displacement estimation offset rate: The above process obtains the corresponding experimental results more intuitively. To further verify the posture estimation effect of each method, a detailed comparison is made. The Data set 2 set is used to compare the hip joint estimation error, knee joint estimation error, ankle joint estimation error and endpoint displacement estimation offset rate of the six methods. Equation (18) refers to

$$S = \frac{f-d}{p_v} \tag{18}$$

where p_v is the actual distance of the track, f is the actual coordinate value of the terminal point, and d is the estimated coordinate of the terminal point.

Curve running motion pose estimation time: This indicator refers to the time taken to complete the curve running motion pose estimation step, the shorter the time, the more efficient the algorithm, Equation (19) refers to

$$e = \sum_{i=1}^{n} t_i \tag{19}$$

where t_i represents the estimated time of the motion posture of the ith curve run.

B. Results and Discussion

The data sampling frequency of the sensor used in this paper is 100Hz, that is, in 1s, there will be one hundred pieces of data each time. To avoid the transition between two actions in a specific split window, a 40% window overlap is used to reduce this effect. After selecting the window to extract the original data, the focus is placed on the extraction of posture and statistical features. In this study, the stochastic gradient descent method described was employed for data augmentation processing to obtain the motion posture angles. The angle between shoulder joint and root node is shown in Fig. 3.

Analysis of Fig. 3 shows that the included angle of shoulder joint in x axis relative to root node changes from 15 ° to 20 °, with a relatively low change range, indicating that the included angle of shoulder joint in x axis relative to root node changes more smoothly. The included angle of shoulder joint in y axis with respect to the root node varies

between 65 ° and 80 °, with a high angle value and a low range of variation, which indicates that the included angle of shoulder joint in Y axis with respect to the root node changes steadily. The included angle of z axis shoulder joint relative to the root node varies from 15 ° to 40 °, with a high variation range, indicating that the included angle of z axis shoulder joint relative to the root node changes unstably.
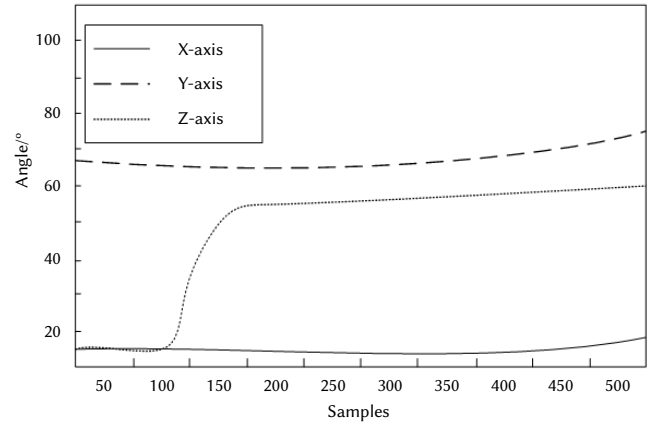
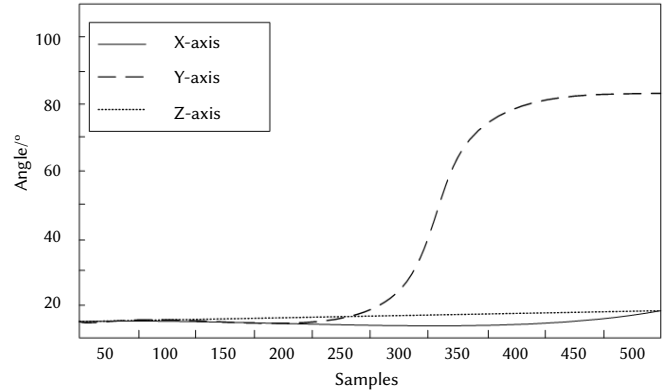Fig. 3. Angle between shoulder joint and root node.

Fig. 4. Included angle between boom and jib.

According to the data in Fig. 4. The included angle between the x axis and y axis boom and the jib varies from 15 ° to 20 °. The angle value is low and the change in posture is small. The included angle between the z axis boom and the jib varies from 15 ° to 80 °. The change of the angle value is unstable, indicating that the included angle between the axial arm and the jib varies greatly.

The changing angle of the included angle between the bones of the left leg within a period of motion is shown in Fig. 5.
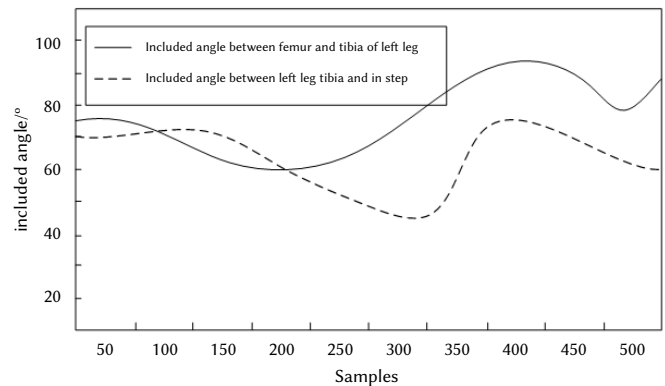
Fig. 5. Included angle between left leg bones in a cycle.

TABLE I. Comparison Results of Hip Joint Estimation

Actual angle°	Proposed method/°	HMCPA [13] method/°	WHMPC[14] method /°	HMTLC[15] method /°	MHDM[16] method /°	HMTPD[17] method /°
25	27	35	28	30	32	18
35	36	36	39	40	40	39
40	41	35	43	45	45	54
25	25	34	26	35	35	42
25	23	32	36	35	26	36
35	35	40	42	40	25	30

Through the analysis of the results in Fig. 5, it can be seen that the included angle between the left leg femur and tibia varies from 57 ° to 90 °, and the included angle between the left leg tibia and instep varies from 45 ° to 70 °. Both of them show irregular changes, and the angle values are kept at a high level, indicating that the included angle between the left leg bones changes greatly during the curve running of the human. After the posture angles of different parts of the athletes are obtained, the curve running posture estimation is developed.

Taking an image in data set 1 as the experimental image, as shown in Fig. 6. The proposed method and five other methods are used to estimate the athlete's posture Fig. 7 in data set1, and the results are shown in Fig. 7.

Fig. 6. Experimental image.

As shown in Fig. 7, the motion posture of the athlete was simulated in three-dimensional space, where the horizontal and vertical coordinates were based on the spatial coordinate system. The differences in the estimation performance between the comparative method and the proposed method have been highlighted in red. The posture angle obtained by the proposed method is consistent with that of actual athletes, which shows that the method can accurately estimate the motion posture. However, the method in HMCPA [13] has deviation for left and right elbow joint and knee joint posture estimation, the method in WHMPC [14] has deviation for knee joint posture estimation, and the method in HMTLC [15] has deviation for left and right elbow joint and knee joint posture estimation, which is the largest deviation among the six methods. The method in MHDM [16] and the method in HMTPD [17] both have deviations in elbow posture estimation. To sum up, the five methods have different degrees of estimation bias, and the posture estimation effect is poor. This is because the posture changes involved in curve motion are complex, encompassing variations in multiple directions and angles, and both the speed and posture of posture changes can vary over time. These complexities with the changes may lead to significant posture estimation errors when using comparative methods. The comparison results of hip joint estimation effects of six methods are shown in Table I.
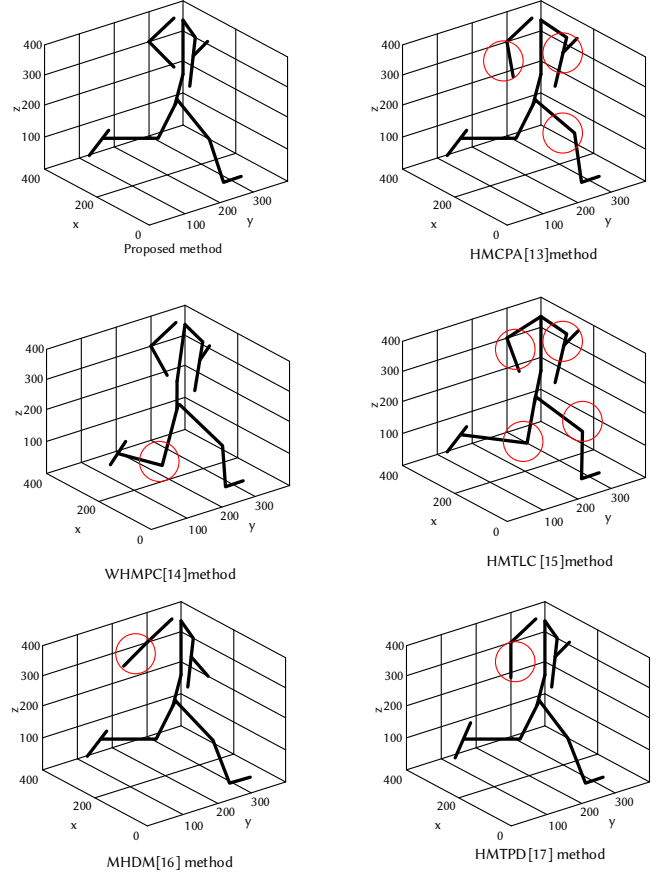

Fig. 7. Comparison of motion posture estimation effects.

In curve motion, the hip joint angle in the human tends to be concentrated in the range of 25°, 35°, and 40°. Therefore, selecting these angles can better adapt to real-world situations. Additionally, choosing these angle ranges can better capitalize on the strengths of various methods. According to the data in Table 1.When the actual angle of the hip joint is 40 °, the hip joint estimated by the proposed method is 42 °, with a difference of 1 °, 4 ° lower than the method in HMCPA [13], 2 ° lower than the method in WHMPC [14], 4 ° lower than the method in HMTLC [15], 4 ° lower than the method in MHDM [16], and 13 ° lower than the method in HMTPD [17]. It can be seen from the analysis and comparison results that the difference between the hip joint estimation results obtained by the proposed method and the actual angle is the lowest, which indicates that the method has higher accuracy in hip joint estimation.

Table II shows the comparison results of the knee joint estimation effects of the six methods.

In curve motion, the knee joint angles in the human tend to be concentrated in the range of 20°, 40°, 50°, 60°, 62°, and 82°. Therefore, selecting these angles can better adapt to real-world situations. Additionally, choosing these angle ranges can better capitalize on

TABLE II. Comparison Results of Knee Joint Estimation

Actual angle°	Proposed method/°	HMCPA[13] method/°	WHMPC[14] method /°	HMTLC [15] method /°	MHDM[16] method /°	HMTPD [17] method /°
50	51	55	60	62	59	62
60	61	69	69	69	70	71
40	41	48	49	48	42	48
82	83	89	89	88	89	90
62	63	70	68	69	52	72
20	22	30	30	32	33	32

TABLE III. Comparison Results of Ankle Joint Estimation

Actual angle°	Proposed method/°	HMCPA [13] method/°	WHMPC[14] method /°	HMTLC [15] method /°	MHDM[16] method /°	HMTPD [17] method /°
11	10	15	16	18	18	19
10	11	15	18	19	13	18
12	12	17	19	18	19	18
15	16	18	19	17	18	20
22	22	23	21	24	25	25
10	12	13	14	15	14	13

the strengths of various methods. According to the results in Table II. When the actual angle of the knee joint is 82 °, the knee joint estimation result of the proposed method is 83 °, and the difference between them is 1 °, which is lower than 6 °, 6 °, 5 °, 6 ° and 7 °, respectively compared with the method in HMCPA [13], the method in WHMPC [14], the method in HMTLC [15], the method in MHDM [16] and the method in HMTPD [17]. This shows that compared with the experimental comparison method, the knee joint estimation result of the proposed method is closer to the actual angle, and the knee joint estimation accuracy is higher.

The ankle joint estimation results of different methods are shown in Table III.

In curve motion, the ankle joint angles in the human body tend to be concentrated in the range of 11°, 10°, 12°, 15°, 22°, and 10°. Therefore, selecting these angles can better adapt to real-world situations. Additionally, choosing these angle ranges can better capitalize on the strengths of various methods. By analyzing the data in Table 3, it can be known that when the actual ankle angle is 22 °. The ankle joint estimation result of the proposed method is also 22 °, and the difference between the two is 0, 1 ° lower than the method in HMCPA [13], 1 ° lower than the method in WHMPC [14], 2 ° lower than the method in HMTLC [15], 3 ° lower than the method in MHDM [16], and 3 ° lower than the method in HMTPD [17]. This shows that the estimation error of the proposed method is the lowest and the effect is the best, and the proposed method also has good estimation accuracy in the estimation of each detail of each joint angle of the motion posture, and the estimation error is not less than 5 °.

According to the data in Fig. 8. The endpoint offset rate of the proposed estimation method after running is low, basically below 2%, which is lower than the other five methods. When the number of experiments is 8, the offset rate of the proposed method reaches the maximum of 0.7%; When the number of experiments is 7, the offset rate of the method in HMCPA [13] reaches the maximum value of 5.9%; When the number of experiments is 8, the offset rate of the method in WHMPC [14] reaches the maximum value of 2.7%; When the number of experiments is 6, the offset rate of the method in HMTLC [15] reaches the maximum value of 5.6%; When the number of experiments is 8, the offset rate of the method in MHDM [16] reaches the maximum value of 8.2%; When the number of experiments is 8, the offset rate of the method in HMTPD [17] reaches the maximum value of 4.6%. In summary, the maximum offset rate of the proposed method is 5.2%,

2%, 3.9%, 6.5% and 3.9% lower than that of the method in HMCPA[13], the method in WHMPC[14], the method in HMTLC[15], the method in MHDM [16] and the method in HMTPD[17], respectively. Compared with the experimental comparison method, the proposed method cannot only estimate the current motion angle, but also accurately estimate the changes of each joint azimuth angle of human motion.
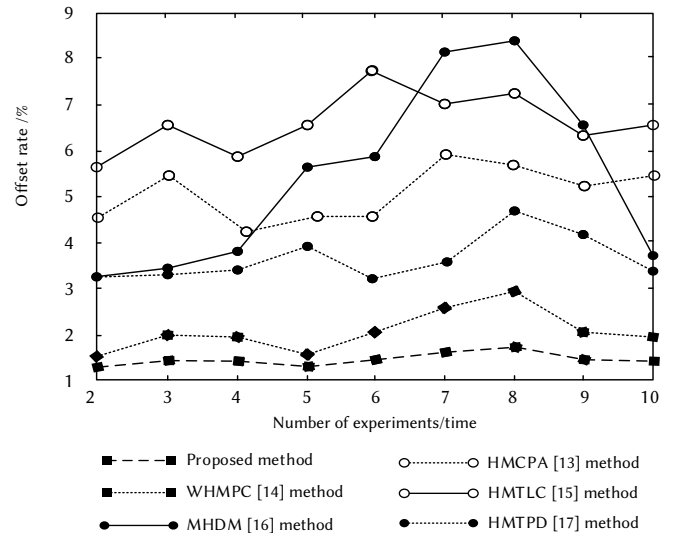

Fig. 8. Comparison results of end point displacement offset rate.

The results of the comparison of the curve running motion posture estimation times for the six methods are shown in Table IV.

According to the data in Table IV. The mean value of curve running motion posture estimation time for the proposed method is 0.65s. The mean value of curve running motion posture estimation time for the method of HMCPA[13] is 1.42s. The mean value of curve running motion posture estimation time for the method of WHMPC[14] is 2.18s. The mean value of curve running motion posture estimation time for the method of HMTLC[15] is 1.52s. The mean value of curve running motion posture estimation time for the method of MHDM[16] is 2.64s. The mean value of curve running motion posture estimation time for the method of HMTPD[17] is 1.59s.The comparison results show that the estimation time of the proposed method is the shortest, which is 0.77s, 1.53s, 0.87s, 1.99s, and 0.94s lower than the methods

TABLE IV. Comparison Results of Curve Running Motion Posture for Estimated Time

Number of experiments	Proposed method/°	HMCPA [13] method/°	WHMPC[14] method /°	HMTLC [15] method /°	MHDM[16] method /°	HMTPD [17] method /°
1	0.55	1.22	2.55	1.25	2.55	1.55
2	0.63	1.36	2.63	1.47	2.86	1.23
3	0.64	1.25	2.47	1.88	2.63	1.63
4	0.74	1.42	1.86	1.63	2.87	1.42
5	0.71	1.44	2.36	1.84	2.49	1.69
6	0.69	1.56	1.25	1.63	2.63	1.72
7	0.88	1.32	2.17	1.28	2.58	1.76
8	0.49	1.64	2.36	1.47	2.47	1.52
9	0.58	1.71	2.78	1.56	2.36	1.99
10	0.61	1.23	1.36	1.23	2.99	1.37

of HMCPA[13], WHMPC [14], HMTLC[15], MHDM[16], and HMTPD[17], respectively, indicating that the estimation time of the proposed method is shorter and the proposed method is more efficient.

IV. Conclusion

Based on the research background of curve running posture estimation, a method of curve running posture estimation based on nano-biosensor and machine learning is designed. The experimental results show that the posture angle obtained by the proposed method is consistent with that of actual athletes, which shows that the method can accurately estimate the motion posture. The difference in hip joint estimation error is 1°, the difference in knee joint estimation error is 1°, the difference in ankle joint estimation error is 0°, and the maximum deviation rate is only 0.7%. The proposed method has important practical value in the field of athletic training, providing more accurate training and competition data for athletes. Although the proposed method has higher accuracy in estimating motion postures and can overcome the limitations of traditional estimation methods, the efficiency of various estimation methods has not been verified in the experimental process. The limitation of this study is that the experimental results provided may come from a smaller sample size. To ensure the reliability and universality of the proposed method, further experiments with larger scale and more diverse samples are needed. Therefore, in the future, it is necessary to evaluate the performance of this method in real scenes, including the impact of various factors (such as lighting conditions, dynamic motion, and different body types) on estimation accuracy.

References

[1] T. Paolo, K. Rodger, M. Alena, "Maximum-speed curve-running biomechanics of sprinters with and without unilateral leg amputations," *Journal of Experimental Biology*, vol. 219, no. 6, pp. 851–858, 2016.

[2] S. Sasaki; Chinthaka P, "Head posture estimation by deep learning using 3-D point cloud data from a depth sensor," *IEEE Sensors Letters*, vol.5, no. 7, pp. 1-4, 2021.

[3] A. Rajendran, S. Sethuraman, "A Survey on Yogic Posture Recognition," *IEEE Access*, vol. 11, pp. 11183-11223, 2023.

[4] M. Takuto, K. Takahiro, K. Toshihiro, M. Tetsuro, K.Kenji, "Three-dimensional posture estimation of robot forceps using endoscope with convolutional neural network," *The International Journal of Medical Robotics and Computer Assisted Surgery*, vol. 16, no. 2, pp. e2062, 2020.

[5] J. Lee, K. Park, Y. Kim, "Deep learning-based device-free localization scheme for simultaneous estimation of indoor location and posture using FMCW radars," *Sensors*, vol. 22, pp. 4447, 2022.

[6] X. Jiang, Z. Hu, S. Wang, Y. Zhang, "A Survey on artificial intelligence in posture recognition," , vol. 137, no. 1, pp. 35–82, 2023.

[7] M. Marcato, S. Tedesco, C. O'Mahony, B. O'Flynn, P. Galvin, "Machine learning based canine posture estimation using inertial data," *PLoS ONE*, vol. 18, no. 6, pp. e0286311, 2023.

[8] M. Lee, Y. Chen, C. Tsai, "Deep Learning-Based Human body posture recognition and tracking for unmanned aerial vehicles," *Processes*, Vol. 10, no. 11, pp. 2295, 2022.

[9] Y. Peng, C. He, H. Xu, "Attachable inertial device with machine learning toward head posture monitoring in attention assessment," *Micromachines*, vol. 13, no. 12, pp. 2212, 2022.

[10] R. Prashant, Kane.L, G.Mrinal, A.Jindal, S. Sehgal, "A review on vision-based hand gesture recognition targeting RGB-Depth sensors," *International Journal of Information Technology & Decision Making*, Vol. 22, no. 1, pp. 115-156, 2023.

[11] D. Kishore, S. Bindu, N. Manjunath, "Estimation of yoga postures using machine learning techniques," *International Journal of Yoga*, vol. 15, no. 2, pp. 137-143, 2022.

[12] F. Sanghavi, O. Jinadu, V. Oludare, K. Panetta, L. Kezebou, S. Roberts, "An individualized machine learning approach for human body weight estimation using smart shoe insoles," *Sensors*, vol. 23, no. 17, pp. 7418, 2023.

[13] S. Shimada, V. Golyanik, W. Xu, Pérez, P. C. Theobalt, "Neural monocular 3d human motion capture with physical awareness," *ACM Transactions on Graphics*, vol. 40, no. 4, pp. 1-15, 2021.

[14] L. Gao, G. Zhang, B. Yu, Z.Qiao, J.Wang, "Wearable human motion posture capture and medical health monitoring based on wireless sensor networks," *Measurement*, vol. 166, no. 4, 108252, 2020.

[15] C. Liu, A. Wang, C. Bu, W.Wang, H.Sun, "Human motion tracking with less constraint of initial posture from a single RGB-D sensor," *Sensors*, vol.21, no.9, pp. 3029, 2021.

[16] S. Liu, J. Zhang, G. Li, R.Zhu, "A wearable flow-MIMU device for monitoring human dynamic motion," *IEEE Transactions on Neural Systems and Rehabilitation Engineering*, vol. 28, no.3, pp. 637-645, 2020.

[17] L. Chen, S. Li, "Human motion target posture detection algorithm using semi-supervised learning in internet of things," *IEEE Access*, vol.9, pp. 90529-90538, 2021.

[18] H. Q. Awla, S. W. Kareem, A. S. Mohammed, "A comparative evaluation of Bayesian networks structure learning using Falcon optimization algorithm," *International Journal of Interactive Multimedia and Artificial Intelligence*, vol. 8, no. 2, pp. 81-87, 2023.

[19] Z. Lv, J. Mauri, H. Song, "Editorial rgb-d sensors and 3d reconstruction," *IEEE Sensors Journal*, vol. 20, no. 20, pp. 11751-11752, 2020.

[20] H. Cha, H. Ji, J. Song, "Robust and autonomous stereo visual-inertial navigation for non-holonomic mobile robots," *IEEE Transactions on Vehicular Technology*, vol. 69, no. 9, pp. 9613-9623, 2020.

[21] P. Cheng, J. Wang, X. Zeng, P. Bruniaux, X. Tao, "Motion comfort analysis of tight-fitting sportswear from multi-dimensions using intelligence systems," *Textile Research Journal*, vol. 92, no. 11, pp. 1843-1866, 2022.

[22] G. Moon, J. Choi, C. Lee, Y. Oh, D. Kim, "Machine learning-based design of meta-plasmonic biosensors with negative index metamaterials," *Biosensors & Bioelectronics,* vol.164, no. 5786, pp. 112335, 2020.

[23] R. Ghosh, O. Smadi, "Automated detection and classification of pavement distresses using 3d pavement surface images and deep learning," *Transportation Research Record*, vol. 2675, no. 9, pp. 1359-1374, 2021.

[24] Z. Wang, L. Zhang, X. Feng, M. Liu, "Intelligent human body posture recognition and its comparative study," *Journal of Physics: Conference Series*, vol. 1894, no.1, pp. 012053-012066, 2021.

[25] N. Nishida, T. Izumiyama, R. Asahi, F. Jiang, T. Sakai, "Analysis of

individual differences in pelvic and spine alignment in seated posture and impact on the seatbelt kinematics using human body model," *PLoS ONE*, vol.16, no.7, pp. e0254120, 2021.

[26] Y. Wang, Y. He, Z. Zhu, "Study on fast speed fractional order gradient descent method and its application in neural networks," *Neurocomputing*, vol. 489, no. 1, pp. 366-376, 2022.

[27] X. Li. H. Jiao, D. Li, "Intelligent medical heterogeneous big data set balanced clustering using deep learning," *Pattern Recognition Letters*, vol. 138, pp. 548-555, 2022.

[28] C. Frederick, S. Villar, Z. Michalopoulou, "Seabed classification using physics-based modeling and machine learning," *The Journal of the Acoustical Society of America*, vol. 148, no. 2, pp. 859-872, 2020.

[29] E. Chumacero-Polanco, J. Yang, "Validation of an ankle-hip model of balance on a balance board via kinematic frequency-content," *Gait & Posture*, vol. 82, no. 11, pp. 313-321, 2020.

[30] J. Gao, C. Ma, H. Su, S. Wang, X. Xu, J. Yao, "Research on gait recognition and prediction based on optimized machine learning algorithm," *Journal of Biomedical Engineering*, vol.39, no.1, pp. 103-111, 2022.

[31] B. Huang, O. Lilienfeld, "Quantum machine learning using atom-in-molecule-based fragments selected on the fly," *Nature Chemistry*, vol. 12, no. 10, pp. 1-7, 2020.

[32] W. Zhu, "Classification accuracy of basketball simulation training system based on sensor fusion and bayesian algorithm," *Journal of Intelligent and Fuzzy Systems*, vol. 39, no. 4, pp. 5965-5976, 2020.

[33] Y. Chen, Li. S, "Monocular depth image mark-less pose estimation based on feature regression," *Journal of System Simulation*, vol. 32, no. 2, pp. 269-277, 2020.

[34] T. Lin, M. Maire, S. Belongie, J. Hays, P. Perona, D. Ramanan, et al., "Microsoft COCO: common objects in context," in Computer Vision – ECCV 2014, *Lecture Notes in Computer Science*, vol. 8693. Springer, Cham, 2014.

Haitao Yang

Haitao Yang received his Master's degree from Hebei Normal University. He is an associate professor with Beijing University of Technology. His research interests include smart sports and basketball.

S. P. Raja

S. P. Raja is born in Sathankulam, Tuticorin District, Tamilnadu, India. He completed his schooling in Sacred Heart Higher Secondary School, Sathankulam, Tuticorin, Tamilnadu, India. He completed his B. Tech in Information Technology in the year 2007 from Dr. Sivanthi Aditanar College of Engineering, Tiruchendur. He completed his M.E. in Computer Science and Engineering in the year 2010 from Manonmaniam Sundaranar University, Tirunelveli. He completed his Ph.D. in the year 2016 in the area of Image processing from Manonmaniam Sundaranar University, Tirunelveli. His area of interest is image processing and cryptography. He is having more than 14 years of teaching experience in engineering colleges. Currently he is working as an Associate Professor in the school of Computer Science and Engineering in Vellore Institute of Technology, Vellore, Tamilnadu, India.

Xiaoming Wu

Xiaoming Wu received his Bachelor of Education degree from Beijing Sports University. He is a lecturer with Capital Normal University. His research interests include sports teaching and training.

Yu Cao

Yu Cao received her Master's degree from Hebei Normal University. She is an associate professor with Renmin University of China. Her research interests include sports teaching and Tennis.

Yu Wang

Yu Wang received his Bachelor of Education degree from Beijing Sports University, and received his Master's degree in education degree from Hebei Normal University. He is an associate professor in Capital Normal University. His research interests include sports teaching and training.

Bing Li

Bing Li is a lecturer in the Physical Education and Training Faculty at Harbin Sport University. Her research interest is mainly in Physical Education, Winter Sports industry and Physical Management. She has published several research papers in scholarly journals in the above research areas and has participated in several books and foundation projects.